ACS APPLIED MATERIALS & INTERFACES

Research Article

Cite This: ACS Appl. Mater. Interfaces 2018, 10, 35361−35366

www.acsami.org

Unusual Ferroelectricity of Trans-Unitcell Ion-Displacement and Multiferroic Soliton in Sodium and Potassium Hydroxides

Yangyang Ren,[†] Shuai Dong,[‡] and Menghao Wu*[,†]

[†]School of Physics, Huazhong University of Science and Technology, Wuhan 430074, Hubei, China

[‡]School of Physics, Southeast University, Nanjing 211189, Jiangsu, China

Supporting Information

ABSTRACT: We show the first-principles evidence of a hitherto unreported type of ferroelectricity with ultralong ion-displacement in sodium and potassium hydroxides. Even a small number of proton vacancies can completely change the mode of proton-transfer from intra-unitcell to trans-unitcell, giving rise to multiferroic soliton with "mobile" magnetism and a tremendous polarization that can be orders of magnitude higher compared with most perovskite ferroelectrics. Their vertical polarizations of thin-film are robust against a depolarizing field, rendering various designs of two-dimensional ferroelectric field-transistors with nondestructive read-out and ultrahigh on/off ratio via sensing the switchable metallic/insulating state.

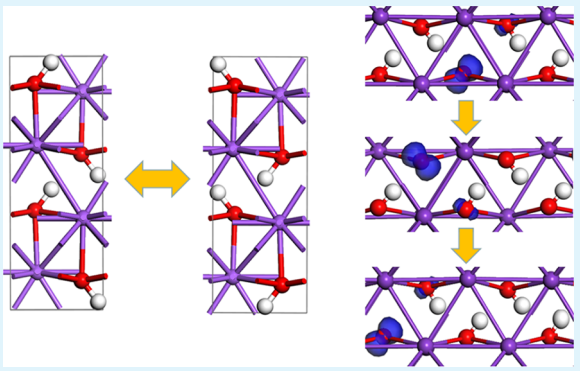

KEYWORDS: *hydrogen-bonded ferroelectrics, trans-unitcell ion-displacement, multiferroic soliton, sodium and potassium hydroxides, 2D ferroelectric field-transistors, ab initio calculations*

INTRODUCTION

Ferroelectric (FE) materials are polar substances with spontaneous electric polarizations that can be switched by an external electric field, which are indispensable for electronics, micromechatronics, and electro-optics. Traditional FEs such as pervoskites[1] have already found a variety of commercial uses, such as nonvolatile memories,[2] piezoelectric actuators, thermal sensors, light modulators, and so on, but still often include toxic lead or rare metals such as bismuth, niobium, or tantalum as the component elements. Moreover, in their ultrathin films, FE perpendicular to the film surface is suppressed by the depolarizing field and will disappear below film thicknesses (like 24 Å in $BaTiO_3$, 12 Å in $PbTiO_3$).[3,4] After all, the displacements of metal ions during FE switching are within 0.5 Å and can be diminished by the depolarizing field. To resolve this issue for the high-density integration of nonvolatile memories, a variety of new FE systems have been explored recently, including FE based on emerging types of two-dimensional (2D) van der Waals materials as summarized in our recent review.[5]

In this paper, we will focus on a prototypical strong base with industrial and niche applications: sodium and potassium hydroxides, which are partially ionic and partially hydrogen-bonded solids as the hydroxyl groups OH^- form hydrogen-bonded networks. However, it has not yet been noticed that FE may be induced by proton-transfer in the hydrogen-bonded network of NaOH and KOH. In such proton-transfer of FE[6−10] where polarity can be formed spontaneously for the direction preference of hydrogen bonding even in one-dimension (1D),[6] steric hindrance or high energy barriers during switching can be avoided and strong hydrogen bonds may give rise to high Curie temperature. Through first-principles calculations, we predict the existence of robust proton-transfer FE with considerable polarization in NaOH and KOH, which enable mass production compared with traditional FE. Moreover, a new mode of FE switching with trans-unitcell ion-displacement may emerge upon a small number of proton vacancies, giving rise to a tremendous polarization and multiferroic soliton with mobile magnetic moments. Their thin-films possess vertical polarizations that are robust against the depolarizing field, which can be used as the FE field-transistor for nonvolatile control of on/off state for 2D materials.

METHODS

The theoretical calculations are performed based on density functional theory (DFT) methods implemented in the Vienna Ab initio Simulation Package (VASP 5.3.3) code.[11,12] The generalized gradient approximation in the Perdew−Burke−Ernzerhof (PBE)[13] form for the exchange and correlation potential, together with the projector-augmented wave[14] method, are adopted. In particular, PBE-D2 functional of Grimme[15] is used to account for the van der Waals interaction. The kinetic energy cutoff is set to be 520 eV, and computed forces on all atoms are less than 0.001 eV/Å after the geometry optimization. For electronic band-structure computation,

Received: July 16, 2018
Accepted: September 24, 2018
Published: September 24, 2018

DOI: 10.1021/acsami.8b11971
ACS Appl. Mater. Interfaces 2018, 10, 35361−35366

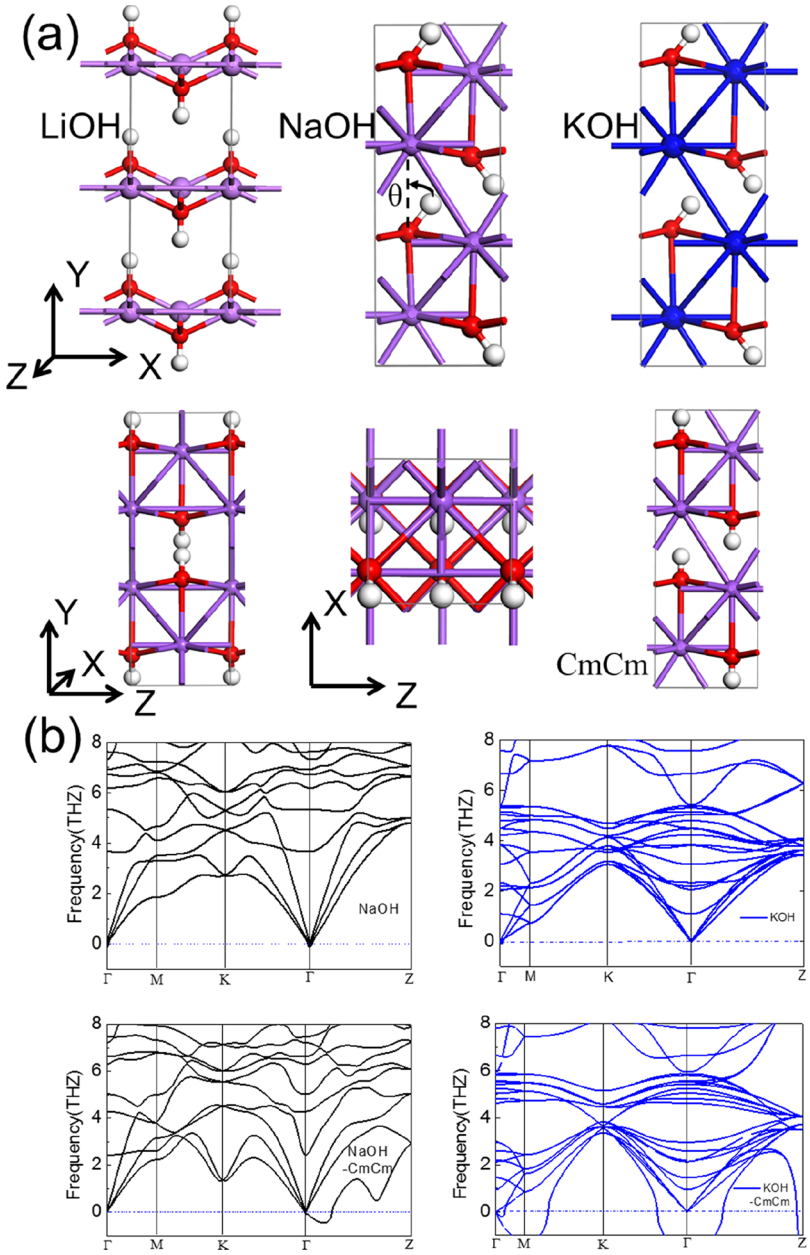

Figure 1. (a) Geometric structure of LiOH, NaOH, and KOH, where pink, purple, blue, red, white spheres denote Li, Na, K, O, H atoms, respectively. (b) Phonon dispersions of NaOH and KOH for polar (ground) and nonpolar (CmCm) states.

the Brillouin zone is sampled using 2 × 6 × 6 and 4 × 8 × 4 *k*-point grid in the Monkhorst−Pack scheme.[16] The Berry phase method is employed to evaluate crystalline polarization,[17] and the FE switching pathway is obtained by using the nudged elastic band (NEB) method.[18] The phonon band structure was calculated using density functional perturbation theory (DFPT).[19] All performed DFPT calculations were started from the fully relaxed structures.

RESULTS AND DISCUSSION

The optimized geometric structures of LiOH, NaOH, and KOH are displayed in Figure 1a, based on previous infrared spectra and proton nuclear magnetic resonance studies.[20,21] Here, the structure of LiOH possesses a highly symmetrical group of *P*4/*nmm* where the −OH bonds are aligned parallel along the −*y* direction, whereas for the ground state of NaOH and KOH, the direction of −OH bonds deviate from the −*y* axis by angles θ = 39.3 and 43.6°, respectively. As a result, polar Ccm21(C2V-12) structures are formed, which are respectively 0.075 and 0.14 eV/f.u. lower than the symmetrical CmCm state where the −OH bonds are aligned parallel along the −*y* direction. Because of the proton deviation, all the −OH groups form into bundles of hydrogen-bonded chains, where the bond lengths of hydrogen bond O···H in NaOH and KOH are, respectively, 1.76 and 1.86 Å. The phonon spectra of the polar ground state and nonpolar phase for NaOH and KOH are plotted in Figure 1b, where the imaginary soft optical modes of the nonpolar phase indicate the spontaneous symmetry-breaking below the Curie temperature. Meanwhile, the dynamical stability of the polar ground state without imaginary frequency in phonon dispersion is further verified for both NaOH and KOH.

The symmetry-breaking induced by proton deviations in NaOH and KOH may give rise to FE, as long as the polarization is switchable and the system is insulating.

DOI: 10.1021/acsami.8b11971
ACS Appl. Mater. Interfaces 2018, 10, 35361−35366

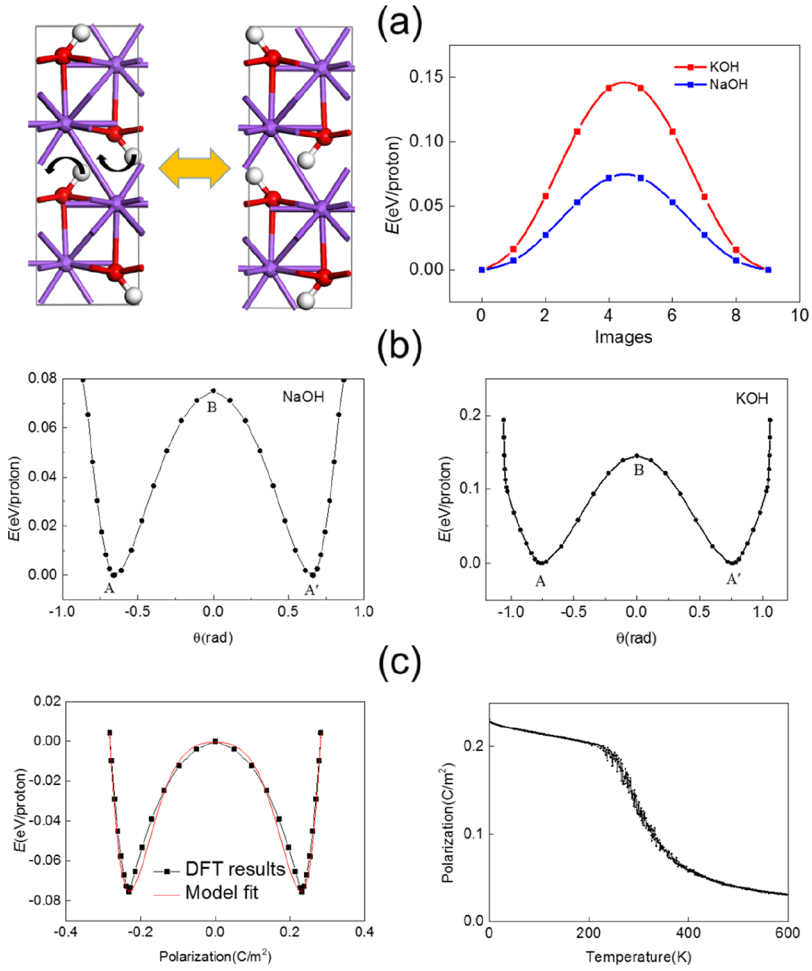

Figure 2. (a) FE switching pathway upon swirling of −OH bonds. (b) Double-well potential of NaOH and KOH vs the deviation angle θ of −OH. (c) Double-well potential of NaOH vs the polarization, and temperature dependence of polarization obtained from Monte Carlo simulations.

According to our calculations, the band gaps of NaOH and KOH are both larger than 6 eV (see Figure S1). If the angle between −OH and the y axis is able to swirl from $-\theta_{max}$ to θ_{max}, the switchable bulk polarization of NaOH and KOH will be, respectively, 23.2 and 17.6 $\mu C/cm^2$, comparable to perovskite FE such as $BaTiO_3$. The energy profiles of the FE switching pathway as a function of step number are plotted in Figure 2a using the NEB method, with the angle between −OH and the y axis swirling from $-\theta_{max}$ to θ_{max}. The obtained switching barrier for NaOH and KOH are, respectively, 0.075 and 0.14 eV/f.u., which may be even lower if the nuclear quantum effect of protons is taken into account. The existence of FE in NaOH and KOH can be further verified by the anharmonic double-well potential versus the deviation angle of −OH in Figure 2b, where the barrier of the double-well potential is consistent with the results obtained by NEB calculations.

Alternatively, those systems can be described by the Landau theory. Here, NaOH is selected as the example for study, where the potential energy is expressed in the Landau−Ginzburg expansion

$$E = \sum_i \frac{A}{2}(P_i^2) + \frac{B}{4}(P_i^4) + \frac{C}{6}(P_i^6) + \frac{D}{2}\sum_{\langle i,j\rangle}(P_i - P_j)^2 \quad (1)$$

which can be viewed as the Taylor series of local structural distortions with a certain polarization defined at each cell P_i. As shown in Figure 2c, the first three terms are associated with the energy contribution from the local modes up to the sixth order, which can well describe the anharmonic double-well potential. The last term captures the coupling between the nearest local modes, which can be obtained by mean-field theory within the nearest-neighbor interaction. The fitted parameters A, B, C, and D turn out to be, respectively, −0.5466, −288.58, 5718.85, and 0.9322. With the effective Hamiltonian and parameters, Monte Carlo simulation is used to investigate the phase transition. Its Curie temperature over 300 K is obtained, which accords with our results of molecular dynamics simulation at 300 K shown in Figure S2.

Besides the swirling of −OH bonds, the hopping of protons may induce another type of FE. As shown in Figure 3a, if the protons are able to simultaneously hop to adjacent O atoms along the hydrogen bonds, the switchable polarization will be 26.1 and 22.6 $\mu C/cm^2$, respectively, for NaOH and KOH. According to our NEB calculation, the hopping barriers are, respectively, 0.23 and 0.28 eV, larger than the −OH swirling barrier. As all the −OH groups form into bundles of quasi-1D hydrogen-bonded chains in NaOH and KOH crystals, a model of a 1D hydrogen-bonded chain is built in Figure 3b. Herein, the proton hopping may be prohibited in the perfect crystal but accessible with proton vacancy: for a proton vacancy

DOI: 10.1021/acsami.8b11971
ACS Appl. Mater. Interfaces 2018, 10, 35361−35366

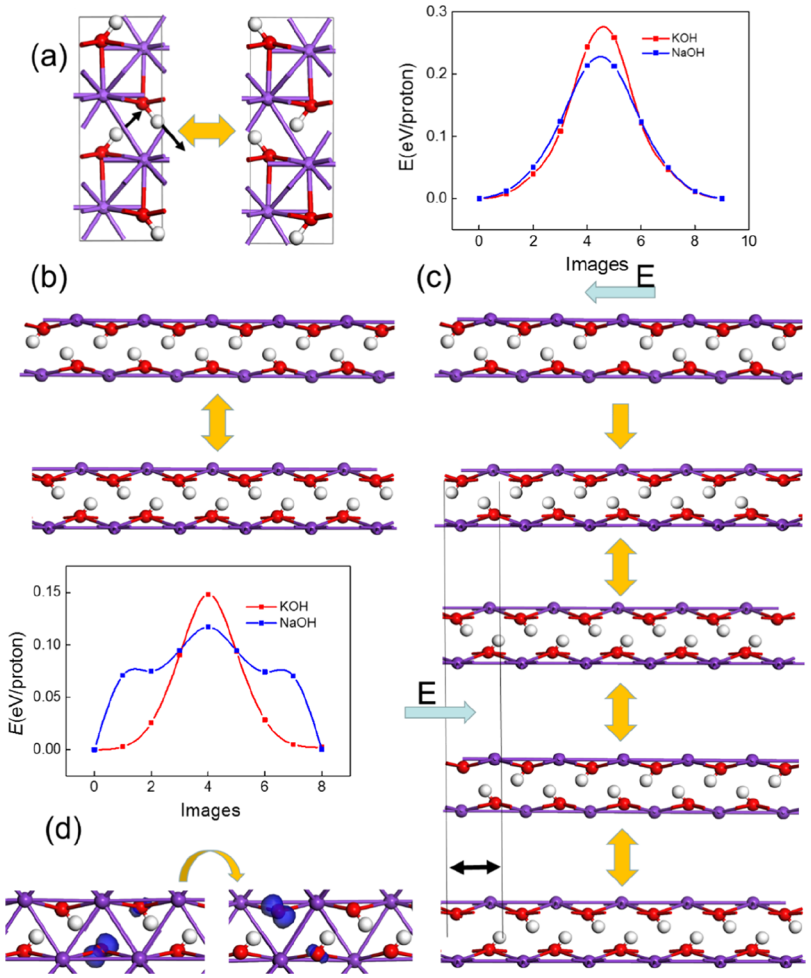

Figure 3. (a) FE switching pathway by proton hopping in NaOH and KOH. (b) Model of proton-transfer along the 1D hydrogen-bonded chain without vacancy. (c) Model of proton-transfer along the 1D hydrogen-bonded chain with one proton vacancy and its FE switching pathway. (d) Hopping pathway of a proton vacancy, where the spin density distribution is plotted in blue.

hopping to its adjacent hydrogen-bonded O atom, the energy barrier is 0.12 and 0.15 eV, respectively, in NaOH and KOH, much lower than the simultaneous hopping barrier of protons without vacancy. It is known that proton-transfer in a hydrogen-bonded chain subjected to an appropriate electrostatic field may behave as a soliton.[22,23] Upon an electric field, the vacancy will be driven to one end of the chain and stop at the interface between electrodes and NaOH/KOH if the electrodes are proton-insulating; similarly, it will be driven to the other end when the electric field is reversed, as shown by the successive trans-unitcell proton-transfer mode in Figure 3c. Here, the bulk property is completely changed by just one vacancy, as the displacement of all protons upon FE switching will be prolonged by half of a periodic length along the chain. The switchable polarization will be, respectively, 72.5 and 57.8 $\mu C/cm^2$ with one proton vacancy for each hydrogen-bonded chain in NaOH and KOH. If there are N vacancies along each chain, theoretically the transfer distance of each proton upon FE switching will be further greatly enhanced, and the switchable polarization will be, respectively, $23.2 + 49.3N$ and $17.6 + 40.2N$ $\mu C/cm^2$ for NaOH and KOH, which can be inconceivable values even to unlimited large: even if only 0.1% protons are missing in a cubic NaOH crystal with size ~1 μm, N = ~6 and the polarization of $NaOH_{0.999}$ will be ~300 $\mu C/cm^2$. Moreover, each proton vacancy induces a magnetic moment of 1 μ_B mainly distributed around the O atom with no proton bonded around (see the spin density distribution around the proton vacancy in Figure 3d), which will follow the migration of vacancy along the hydrogen-bonded chain. As a result, the soliton will be multiferroic with "mobile" magnetism along the chain, which also renders a coupling between FE and magnetism for efficient data reading and writing.

It is known that for ultrathin films of traditional FE, the vertical polarization is suppressed by the depolarizing field and will disappear or switch in-plane below critical thicknesses. However, for both NaOH and KOH the polarization is aligned along the direction of hydrogen-bonded chains, which can be hardly diminished or turned to other directions. If the chain direction is set as the vertical direction for a six-layer KOH thin-film, the polarization will be 0.3×10^{-10} C/m, much larger than the vertical polarization obtained in previously predicted 2D FE (e.g., 0.02×10^{-10} C/m for bilayer boron nitride,[24] 0.11×10^{-10} C/m for intercalated phosphorene bilayer[25]). The polarization will be switchable at ambient condition as the switching barrier in the thin-film is lowered to 0.06 eV/proton (see the structure and pathway in Figure 4a). Moreover, the polarization can be even greatly enhanced with a small amount of proton vacancies, which also induce electrical-tunable magnetism. It can be used as the FE dielectrics on 2D materials for nonvolatile control of a field-effect transistor,[26] as

DOI: 10.1021/acsami.8b11971
ACS Appl. Mater. Interfaces 2018, 10, 35361−35366

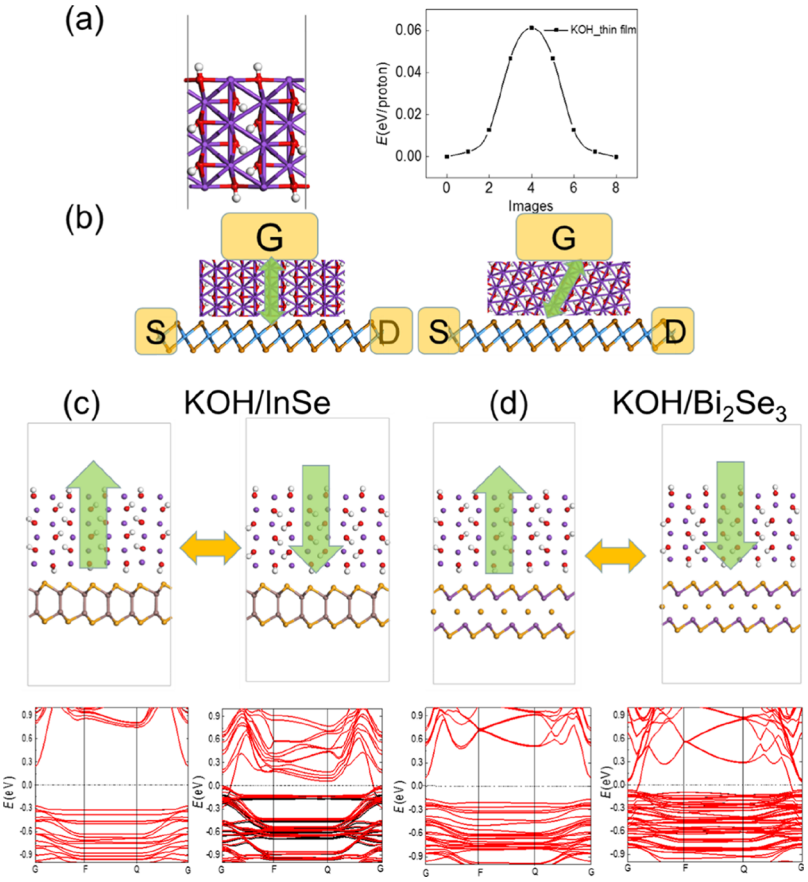

Figure 4. (a) KOH thin-layer and vertical FE switching pathway. (b) Designs of 2D FE field-effect transistors based on (c) KOH/InSe and (d) KOH/Bi_2Se_3 heterostructures. Green arrows denote the polarization direction of the KOH thin-film.

shown in Figure 4b: electrons accumulate as the FE polarization is directed toward 2D materials, and depletes as the polarization is directed opposite. As NaOH and KOH are uniaxial FE along the chain direction, the in-plane polarization can also be switched upon vertical FE switching if the chain orientation is set with a tilted angle from the vertical direction. Herein, the 2D InSe and Bi_2Se_3 monolayers that have been experimentally verified to be semiconductors with high electron mobility[27] are chosen as two examples for design, also because of their perfect lattice match with KOH for DFT calculations. As shown in Figure 4c,d, both systems of KOH/InSe and KOH/Bi_2Se_3 heterostructures are semiconducting with moderate band gaps when the FE polarizations of KOH point upwards, whereas both become metallic when the FE polarizations switch downwards and toward the 2D materials.[28] The switchable semiconducting/metallic states render an ultrahigh on/off ratio for nondestructive readout via sensing two distinct source−drain resistances.

CONCLUSIONS

In summary, we show the first-principles evidence of robust proton-transfer FE with considerable polarization in NaOH and KOH, which enable commercial mass production. Moreover, even a small number of proton vacancies can change the mode of proton-transfer from intra-unitcell to trans-unitcell, leading to a greatly enhanced polarization because of the prolonged transfer distance: for example, the polarization of a $NaOH_{0.999}$ crystal with size ∼1 μm can be ∼300 $\mu C/cm^2$. A new type of multiferroic soliton with "mobile" magnetic moment can also be formed by proton vacancy, rendering a coupling between FE and magnetism for efficient data reading/writing. The NaOH and KOH thin-film possesses vertical polarizations that are robust against the depolarizing field, which can be used as FE field-transistors for nonvolatile control of insulating/metallic state for 2D materials and hold great promise as multifunctional devices. We note that both NaOH and KOH are hygroscopic, and the polarization will be much reduced when water is adsorbed into the crystal because of disorder. Chemically inert materials such as boron nitride or silicon dioxides can be suitable choices for the protective layer against water. As sodium and potassium hydroxides are a common base in the laboratory, we expect our predictions can advance experimental verifications of their proton-transfer FE and related future applications in nanoelectronics.

ASSOCIATED CONTENT

Supporting Information

The Supporting Information is available free of charge on the ACS Publications website at DOI: 10.1021/acsami.8b11971.

Band structures of NaOH and KOH, and molecular dynamics simulation of NaOH at 300 K (PDF)

AUTHOR INFORMATION

Corresponding Author

*E-mail: wmh1987@hust.edu.cn.

DOI: 10.1021/acsami.8b11971
ACS Appl. Mater. Interfaces 2018, 10, 35361−35366

ORCID

Shuai Dong: 0000-0002-6910-6319

Menghao Wu: 0000-0002-1683-6449

Notes

The authors declare no competing financial interest.

■ ACKNOWLEDGMENTS

We are supported by the National Natural Science Foundation of China (nos. 21573084). We thank Prof. Junming Liu for helpful discussions and Shanghai Supercomputing Center for providing computational resources.

■ REFERENCES

(1) Dawber, M.; Rabe, K. M.; Scott, J. F. Physics of Thin-film Ferroelectric Oxides. *Rev. Mod. Phys.* **2005**, *77*, 1083−1130.

(2) Hong, S.; Auciello, O.; Wouters, D. *Emerging Non-Volatile Memories*; Springer US: Boston, MA, 2014.

(3) Junquera, J.; Ghosez, P. Critical Thickness for Ferroelectricity in Perovskite Ultrathin Films. *Nature* **2003**, *422*, 506−509.

(4) Fong, D. D.; Stephenson, G. B.; Streiffer, S. K.; Eastman, J. A.; Auciello, O.; Fuoss, P. H.; Thompson, C. Ferroelectricity in Ultrathin Perovskite Films. *Science* **2004**, *304*, 1650−1653.

(5) Wu, M.; Jena, P. The rise of two-dimensional van der Waals ferroelectrics. *Wiley Interdiscip. Rev.: Comput. Mol. Sci.* **2018**, *8*, e1365.

(6) Wu, M.; Burton, J. D.; Tsymbal, E. Y.; Zeng, X. C.; Jena, P. Hydroxyl-Decorated Graphene Systems as Candidates for Organic Metal-Free Ferroelectrics, Multiferroics, and High-Performance Proton Battery Cathode Materials. *Phys. Rev. B: Condens. Matter Mater. Phys.* **2013**, *87*, 081406.

(7) Wu, M.; Burton, J. D.; Tsymbal, E. Y.; Zeng, X. C.; Jena, P. Multiferroic Materials Based on Organic Transition-Metal Molecular Nanowires. *J. Am. Chem. Soc.* **2012**, *134*, 14423−14429.

(8) Tu, Z.; Wu, M.; Zeng, X. C. Two-Dimensional Metal-Free Organic Multiferroic Material for Design of Multifunctional Integrated Circuits. *J. Phys. Chem. Lett.* **2017**, *8*, 1973−1978.

(9) Wu, M.; Duan, T.; Lu, C.; Fu, H.; Dong, S.; Liu, J. Proton Transfer Ferroelectricity/Multiferroicity in Rutile Oxyhydroxides. *Nanoscale* **2018**, *10*, 9509−9515.

(10) Horiuchi, S.; Kumai, R.; Tokura, Y. Hydrogen-Bonding Molecular Chains for High-Temperature Ferroelectricity. *Adv. Mater.* **2011**, *23*, 2098−2103.

(11) Kresse, G.; Furthmüller, J. Efficient iterative schemes forab initiototal-energy calculations using a plane-wave basis set. *Phys. Rev. B: Condens. Matter Mater. Phys.* **1996**, *54*, 11169−11186.

(12) Kresse, G.; Furthmüller, J. Efficiency of Ab-Initio Total Energy Calculations for Metals and Semiconductors Using a Plane-Wave Basis Set. *Comput. Mater. Sci.* **1996**, *6*, 15−50.

(13) Perdew, J. P.; Burke, K.; Ernzerhof, M. Generalized Gradient Approximation Made Simple. *Phys. Rev. Lett.* **1996**, *77*, 3865−3868.

(14) Blöchl, P. E. Projector Augmented-Wave Method. *Phys. Rev. B: Condens. Matter Mater. Phys.* **1994**, *50*, 17953−17979.

(15) Grimme, S. Semiempirical GGA-type Density Functional Constructed with a Long-Range Dispersion Correction. *J. Comput. Chem.* **2006**, *27*, 1787−1799.

(16) Monkhorst, H. J.; Pack, J. D. Special Points for Brillouin-Zone Integrations. *Phys. Rev. B: Solid State* **1976**, *13*, 5188−5192.

(17) King-Smith, R. D.; Vanderbilt, D. Theory of Polarization of Crystalline Solids. *Phys. Rev. B: Condens. Matter Mater. Phys.* **1993**, *47*, 1651−1654.

(18) Henkelman, G.; Uberuaga, B. P.; Jónsson, H. A Climbing Image Nudged Elastic Band Method for Finding Saddle Points and Minimum Energy Paths. *J. Chem. Phys.* **2000**, *113*, 9901−9904.

(19) Baroni, S.; de Gironcoli, S.; Dal Corso, A.; Giannozzi, P. Phonons and Related Crystal Properties from Density-Functional Perturbation Theory. *Rev. Mod. Phys.* **2001**, *73*, 515−562.

(20) Busing, W. R. Infrared Spectra and Structure of NaOH and NaOD. *J. Chem. Phys.* **1955**, *23*, 933−936.

(21) Amm, D. T.; Segel, S. L.; Heyding, R. D.; Hunter, B. K. Proton Nuclear Magnetic Resonance and Line Shape Analysis in The Alkali Metal Hydroxides: LiOH, NaOH, KOH, and RbOH. *J. Chem. Phys.* **1985**, *82*, 2529−2534.

(22) Kashimori, Y.; Kikuchi, T.; Nishimoto, K. The Solitonic Mechanism for Proton Transport in a Hydrogen Bonded Chain. *J. Chem. Phys.* **1982**, *77*, 1904−1907.

(23) Stamenković, S.; Žakula, R. B. Solitons in Pseudo One-Dimensional Hydrogen Bonded Ferroelectrics. *Phys. A* **1980**, *102*, 554−560.

(24) Li, L.; Wu, M. Binary Compound Bilayer and Multilayer with Vertical Polarizations: Two-Dimensional Ferroelectrics, Multiferroics, and Nanogenerators. *ACS Nano* **2017**, *11*, 6382−6388.

(25) Yang, Q.; Xiong, W.; Zhu, L.; Gao, G.; Wu, M. Chemically Functionalized Phosphorene: Two-Dimensional Multiferroics with Vertical Polarization and Mobile Magnetism. *J. Am. Chem. Soc.* **2017**, *139*, 11506−11512.

(26) Wu, M.; Dong, S.; Yao, K.; Liu, J.; Zeng, X. C. Ferroelectricity in Covalently functionalized Two-dimensional Materials: Integration of High-mobility Semiconductors and Nonvolatile Memory. *Nano Lett.* **2016**, *16*, 7309−7315.

(27) Bandurin, D. A.; Tyurnina, A. V.; Yu, G. L.; Mishchenko, A.; Zólyomi, V.; Morozov, S. V.; Kumar, R. K.; Gorbachev, R. V.; Kudrynskyi, Z. R.; Pezzini, S.; Kovalyuk, Z. D.; Zeitler, U.; Novoselov, K. S.; Patanè, A.; Eaves, L.; Grigorieva, I. V.; Fal'ko, V. I.; Geim, A. K.; Cao, Y. High Electron Mobility, Quantum Hall Effect and Anomalous Optical Response in Atomically Thin InSe. *Nat. Nanotechnol.* **2017**, *12*, 223−227.

(28) Hong, S.; Nakhmanson, S. M.; Fong, D. D. Screening Mechanisms at Polar Oxide Heterointerfaces. *Rep. Prog. Phys.* **2016**, *79*, 076501.

DOI: 10.1021/acsami.8b11971
ACS Appl. Mater. Interfaces 2018, 10, 35361−35366